NIH Public Access
Author Manuscript
Metallomics. Author manuscript; available in PMC 2013 August 05.

Published in final edited form as:
Metallomics. 2010 March ; 2(3): 211–219. doi:10.1039/b920471g.

Trivalent arsenicals and glucose use different translocation pathways in mammalian GLUT1

Xuan Jiang[1], **Joseph R. McDermott**[2], **A. Abdul Ajees**[3], **Barry P. Rosen**[1,3], and **Zijuan Liu**[2,†]

[1]Departments of Biochemistry and Molecular Biology, Wayne State University, School of Medicine, Detroit, Michigan, USA

[2]Department of Biological Sciences, Oakland University, Rochester, Michigan

[3]Florida International University College of Medicine, Miami, Florida

Summary

Rat glucose transporter isoform 1 or rGLUT1, which is expressed in neonatal heart and the epithelial cells that form the blood-brain barrier, facilitates uptake of the trivalent arsenicals arsenite as $As(OH)_3$ and methylarsenite as $CH_3As(OH)_2$. GLUT1 may be the major pathway for arsenic uptake into heart and brain, where the metalloid causes cardiotoxicity and neurotoxicity. In this paper, we compare the translocation properties of GLUT1 for trivalent $CH_3As(OH)_2$ and glucose. Substitution of Ser^{66}, Arg^{126} and Thr^{310}, residues critical for glucose uptake, led to decreased uptake of glucose but increased uptake of $CH_3As(OH)_2$. The K_m for uptake of $CH_3As(OH)_2$ of three clinically identified mutants, S66F, R126K and T310I, were decreased 4–10 fold compared to native GLUT1. The osmotic water permeability coefficient (P_f) of GLUT1 and the three clinical isolates increased in parallel with the rate of $CH_3As(OH)_2$ uptake. GLUT1 inhibitors Hg(II), cytochalasin B and forskolin reduced uptake of glucose but not $CH_3As(OH)_2$. These results indicate that $CH_3As(OH)_2$ and water use a common translocation pathway in GLUT1 that is different than that of glucose transport.

Keywords

GLUT1; glucose permease; arsenite; monomethylarsenous acid; water translocation pathway; GLUT1 deficiency syndrome (GLUT1-DS)

Introduction

Arsenic is an environmental toxin that ranks first on the EPA's list for toxic substances (http://www.atsdr.cdc.gov/cercla/05list.html). It enters the environment primarily from geochemical sources, although it is introduced anthropogenically as well [1]. The major source of human arsenic exposure is in the food supply and drinking water. Chronic arsenic poisoning via drinking water has been reported in many countries, including Bangladesh, India, China, Chile and United States [2]. In Bangladesh, over 46 million people drink arsenic-contaminated well water that contains as much as 1000-fold more arsenic than the World Health Organization (WHO) limit of 10 ppb [3]. Chronic arsenic exposure has been associated with multiple diseases, including neurological disorders, diabetes mellitus, various cancers and cardiovascular diseases such as coronary artery disease, stroke and peripheral arterial

[†]Corresponding author: Zijuan Liu, Ph.D. Department of Biological Sciences, Oakland University, Dodge Hall 325, 2200 Squirrel Rd., Rochester, MI 48309, USA Phone: 248-370-3554 Fax: 248-370-4225 liu2345@oakland.edu.

NIH-PA Author Manuscript
NIH-PA Author Manuscript
NIH-PA Author Manuscript

NIH-PA Author Manuscript

NIH-PA Author Manuscript

NIH-PA Author Manuscript

disease [4]. However, the mechanisms by which arsenic causes human disease are far from clear.

The initial step in arsenic toxicity is uptake into cells. We have identified two uptake pathways: aquaglyceroporin channels, in particular the liver isoform AQP9, and the glucose permease GLUT1 conduct trivalent $As(OH)_3$ and $CH_3As(OH)_2$ [5, 6], which both have oxidative status of +3. GLUT1, which belongs to the major facilitator superfamily (MFS) [7], facilitates uptake of glucose in many cell types, including neonatal cardiomyocytes, erythrocytes and the endothelial cells that form the blood-brain barrier [8]. We propose that GLUT1 is the major pathway for movement of trivalent inorganic and methylated arsenic into heart and brain, where aquaglyceroporins are not abundantly expressed, and this uptake may contribute to cardiovascular disease and neurotoxicity [9].

In the absence of crystal structure data, most structure/function studies on GLUT1 have been proposed using homology modeling and site-directed mutagenesis. Homology modeling of human GLUT1 based on glycerol phosphate transporter (GlpT) [10] has provided useful predictions on the GLUT1 translocation mechanism. Here we used another GLUT1 homologue, the *E. coli* lactose permease (LacY) [11] to predict an open form model of rGLUT1 to better explain the observation of differential transport of arsenic and glucose (Fig. 1). This model can fit the secondary structure of 12 transmembrane segments (TMs) which have been proposed based on solvent accessibility by cysteine-scanning mutagenesis and affinity labeling assays [12–23]. In addition, GLUT1 was found to have weak water transport activity [24], possibly through a water permeation pathway that is different than the glucose transport pathway [25]. A clinically identified mutation, T310I, which causes a GLUT1-deficiency syndrome (GLUT1-DS) [26], decreases glucose transport but increases water permeation [25], supporting the idea of separate glucose and water pathways. We previously suggested that $As(OH)_3$ could go through the glucose pathway as a cyclic trimer that resembles the glucose molecule [27]. $CH_3As(OH)_2$ and glucose reciprocally inhibited uptake of each other noncompetitively [9], suggesting different binding sites for the two molecules. Here we propose that that $As(OH)_3$ and $CH_3As(OH)_2$ go through the water pathway in GLUT1, and we present data on uptake of $CH_3As(OH)_2$ by wild type and mutant rat GLUT1s expressed in *Xenopus laevis* oocytes that support this proposal. Rat GLUT1 was chosen for this study because it has a higher rate of $CH_3As(OH)_2$ transport than human GLUT1 [9]. Substitutions in residues Ser^{66}, Arg^{126} and Thr^{310} led to a dramatic decrease in glucose transport but a significant increase in permeation of both water and $CH_3As(OH)_2$. Hg(II), cytochalasin B (cytB) and forskolin, inhibitors of glucose transport via GLUTs, reduced glucose transport but had little inhibition on $CH_3As(OH)_2$ transport. These data support our hypothesis that trivalent arsenicals and water share a common translocation pathway that is different from the main glucose pathway.

Experimental Procedures

Oligonucleotide-directed mutagenesis

Mutations in rat GLUT1 were introduced in the plasmid pL2-5-rGLUT1 by site-directed mutagenesis (Stratagene, La Jolla, CA). The sequences of the mutagenic oligonucleotides and amino acid changes are described in Table 1. The mutation was confirmed by sequencing the entire gene using a CEQ2000 DNA sequencer (Beckman Coulter, Fullerton, CA).

Expression of rGLUT1 and mutants in oocytes

Plasmid pL2-5-rGLUT1 and its mutants were linearized with *NotI*. Capped cRNAs were synthesized *in vitro* (mMESSAGE mMACHINE ultra kit, Applied Biosystems, Austin, TX),

NIH-PA Author Manuscript

NIH-PA Author Manuscript

NIH-PA Author Manuscript

and dissolved in distilled water at a final concentration of 0.4 to 0.5 ng/nl. State V and VI defolliculated *X. laevis* oocytes were injected with 50 ng of cRNA of wild type rGLUT1 or its mutants. Control oocytes were injected with 50 nl of water. The oocytes were incubated at 16°C for 3 days in complete ND96 buffer containing 5 mM HEPES, pH 7.5, 96 mM NaCl, 2 mM KCl, 1.8 mM $CaCl_2$, 1 mM $MgCl_2$, 2.5 mM sodium pyruvate, 0.5 mM theophylline, and 2 μg/ml of gentamicin sulphate.

Transport assays

Transport assays for arsenic and glucose in oocytes were performed as described [9]. For assay of $CH_3As(OH)_2$ (a gift from William Cullen, University of British Columbia, Canada) accumulation, groups of 5 to 10 oocytes were incubated in 0.5 ml incomplete ND96 buffer (5 mM HEPES, pH 6.5, 96 mM NaCl, 2 mM KCl, 1.8 mM $CaCl_2$, 1 mM $MgCl_2$) with the indicated concentrations of $CH_3As(OH)_2$ at room temperature. After either 30 or 60 min, as indicated, the reaction was terminated by washing the oocytes 3 times with 0.75 ml of incomplete ND96 buffer. Oocytes were then transferred to 1.5 ml microcentrifuge tube and completely digested with 50 μl 70% nitric acid. Each sample was diluted with 2 ml HPLC grade water (Sigma, St. Louis, MO). Arsenic concentrations were quantified by inductively coupled plasma-mass spectrometry (ICP-MS) (ELAN 9000, PerkinElmer, Norwalk, CT).

For the assays of glucose transport, the oocytes were incubated in 0.5 ml of incomplete ND96 buffer containing 0.5 μCi/ml D-[U-^{14}C] glucose (Perkin-Elmer, Wellesley, MA) and 0.1 mM unlabelled glucose (Sigma, St. Louis, MO) at room temperature for 1 hr. Oocytes injected with rGLUT1 or water (control) were pretreated in the presence or absence of the indicated concentrations of cytB, forskolin, dimethyl sulfoxide (DMSO) or $HgCl_2$ at room temperature for 25 min before initiation of the transport assay. CytB and forskolin were prepared in DMSO. Uptake was terminated by washing the oocytes three times with 0.5 ml incomplete ND96 buffer containing 0.1 mM unlabelled glucose. Individual oocyte was then solubilized with 0.1 ml of 10% SDS, and radioactivity was quantified using a liquid scintillation counter. Each set of transport experiment was repeated at least twice with different batches of oocytes.

Immunological detection of expression of rGLUT1 and its mutants

Oocyte membranes were isolated as described with minor modifications [28]. Briefly, six oocytes were homogenized together in incomplete ND96 buffer by vortexing, followed by centrifugation. The membranes were washed twice with incomplete ND96 and suspended in 0.2 ml the same buffer, solubilized with 5X SDS loading buffer for 10 min at room temperature and separated by SDS-PAGE. Immunoblotting was performed using a commercial anti-GLUT1 primary antibody (Alpha Diagnostic, San Antonio).

Measurement of water osmolarity

Oocytes were incubated for 3 days at 16°C in 205 mosM ND96 medium. P_f was determined by placing oocytes in 1:5 diluted incomplete ND96, with swelling recorded using a microscope (Nikon LABOPHOT-2) and camera system (SPOT PURSUIT Diagnostic Instruments Inc.) at 10 sec intervals continuously for 1 min. The water permeation coefficient (P_f) was calculated as reported [29].

Statistical Analysis

Quantitative results are shown as the mean ± standard deviation. Statistical analyses were performed by Student's t test for paired data between control and mutants. P values <0.05 were considered significant. For each assay, at least two animals and totally eight samples were used. One group of assay (four samples) is presented.

NIH-PA Author Manuscript

NIH-PA Author Manuscript

NIH-PA Author Manuscript

Structural modeling of rGLUT1

A rat GLUT1 homology inward-facing model was constructed using the three dimensional structure of lactose permease of *Escherichia coli* (LacY and PDB code: 1PV6) as a template using Modeller 9v6 [30]. The outward-facing model was constructed based on the LacY model of Smirnova *et al.* [11]. The final model was subject to energy minimization using CHARMM [31]. Initial energy minimization was done with a steep descent algorithm (100 steps) and followed by adopted basis Newton-Raphson method (1000 steps). The Cα-Cα distance in the rGLUT1 outward model was comparable to LacY outward model proposed by Irina Smirnova *et al.* (Table 2). This rGLUT1 outwardly-facing model is also consistent with the secondary model proposed by Mueckler and Makepeace [23]. The channel was calculated using CAVER [32], and graphical images were rendered with PyMOL [33].

Results

Glucose and arsenic transport in wild type and mutant rGLUT1

Structure-function relationships in GLUT1 have been studied by site-directed mutagenesis [12–23]. Five residues, including Gln^{161}, Gln^{282}, Gln^{283}, Thr^{310} and Asn^{317}, have been predicted to form hydrogen bonds with glucose in the pyranose form [23]. All five are highly conserved in human GLUT1 through human GLUT5, indicating that they might play a similar role in formation of hydrogen bonds. We examined the effect of substitutions of these five residues and eight missense clinical GLUT1-DS mutations: S66F [34], G91D [35], R126H [36], R126L [34], E146K [34], K256V [34], T310I [37] and R333W [34] on glucose and arsenic uptake in rGLUT1. GLUT1-DS causes a decrease rate of glucose transport through the blood-brain barrier, resulting in an inadequate energy supply to brain and delayed neurological development [38, 39].

Mutations of each of five putative hydrogen bond donors (Gln^{161}, Gln^{282}, Gln^{283}, Thr^{310}, and Asn^{317}) to alanine had no significant effect on either glucose or $CH_3As(OH)_2$ transport (data not shown), suggesting that elimination of a single hydrogen bond may not be sufficient to influence the initial binding of glucose [40, 41] or $CH_3As(OH)_2$. All eight GLUT1-DS mutants decreased glucose transport. The G91D, E146K, K256V and R333W mutants exhibited reduced uptake of both $CH_3As(OH)_2$ and glucose (data was not shown). In contrast, the S66F and T310I mutants exhibited a 2-fold increase in $CH_3As(OH)_2$ uptake (Fig. 2C and 4C), and the Arg^{126} substitutions R126H and R126L had no effect on $CH_3As(OH)_2$ transport even though they reduced glucose uptake (Fig. 3C). Thus mutations in Ser^{66}, Arg^{126} and Thr^{310} differentially affect glucose and arsenical transport.

To examine their roles in more details, the three residues were replaced by residues of different sizes and hydrophobicity (Table 1). From immunoblotting, in each case the oocyte membrane contained similar amounts of the mutant GLUT1 proteins (Fig. 2A and also found with other mutants in Fig. 3A, 4A, and 8A). Ser^{66} is predicted to be the last amino acid of a large extracellular loop connecting transmembrane sector 1 (TM1) and TM2 [23]. Substitution of Ser^{66} with larger aromatic residues (S66F or S66Y) decreased glucose transport (Fig. 2B), while replacement with residues with larger or smaller sizes (S66C, F, T, Y) resulted in a significant increase in uptake of $CH_3As(OH)_2$ (Fig. 2C).

Arg^{126}, the mutation most frequently found in GLUT1-DS [42], is the last amino acid of the extracellular loop connecting TM3 and TM4 [23], and is predicted to be located near the opening of the primary glucose translocation pathway [42]. Altering Arg^{126} to alanine, histidine, lysine or leucine considerably decreased glucose uptake (Fig. 3B). However, the efficiency of $CH_3As(OH)_2$ uptake by Arg^{126} mutants was found to be Ala < His = Leu = wild type < Lys. Importantly, while the R126K mutant showed a two-fold decrease in glucose accumulation compared with wild type, it exhibited a dramatic increase in

NIH-PA Author Manuscript

NIH-PA Author Manuscript

NIH-PA Author Manuscript

$CH_3As(OH)_2$ transport (Fig. 3C). R126A and R126L were expressed in high amounts, but the amounts of the fully glycosylated form (Fig. 3A, upper band) were reduced, possibly resulting from aberrant trafficking to the plasma membrane, as has been observed with human SGLT1 mutants [43]. R126H was present in lower amounts in the oocyte membrane, perhaps due to improper folding.

Thr^{310} is highly conserved throughout the GLUT family, from GLUT1 to GLUT5. It is predicted to be at or near the exofacial end of TM8 and to participate in formation of the water-accessible glucose translocation pathway [23]. Six different Thr^{310} mutants (T310A, F, I, R, S, V) exhibited increased $CH_3As(OH)_2$ uptake, while three of them, T310F, T310I and T310R, showed decreased glucose uptake (Fig. 4B). The K_m for $CH_3As(OH)_2$ uptake in wild type, S66F, R126K and T310I was determined (Fig. 5). In these assays, background uptake of water-injected oocytes was subtracted from all groups. While the V_{max} values for the wild type and mutants were similar, wild type affinity for $CH_3As(OH)_2$ (K_m = 3.9 mM) is lower than in S66F, R126K or T310I (K_m values of 0.52 mM, 0.4 mM and 1.0 mM, respectively).

GLUT1 inhibitors do not affect $CH_3As(OH)_2$ transport

The docking sites for β-D-glucose and several well-characterized inhibitors have been predicted in the hGLUT1 homology model [40]. CytB and forskolin are inhibitors of glucose permeases. In this model, glucose and forskolin dock near the glucose binding site (Trp^{65}) on the extracellular face of GLUT1. Forskolin can also penetrate the plasma membrane and bind to another site (Phe^{81}) at the intracellular face of the translocation pathway. CytB docks at the intracellular face of the pathway but further toward the membrane than the binding site for forskolin. The effect of these inhibitors on $CH_3As(OH)_2$ uptake was examined (Fig. 6). CytB and forskolin abolished glucose transport compared with the water-injected control (Fig. 6A), but neither inhibitor had an effect on $CH_3As(OH)_2$ transport (Fig. 6B). These results are consistent with our previous observation that cytB and foskolin inhibit glucose but not $CH_3As(OH)_2$ uptake when rGLUT1 was expressed in *S. cerevisiae* [9].

Mercurials bind to cysteine residues (Cys^{429} in GLUT1 [44]) and occlude transport pathways [45]. The effect of 0.2 mM $HgCl_2$ on glucose and $CH_3As(OH)_2$ uptake via rGLUT1 was examined (Fig. 7). Transport of glucose was inhibited by Hg(II) (Fig. 7A), while $CH_3As(OH)_2$ uptake decreased largely unaffected (Fig. 7B). Again, these results indicate the glucose pathway in GLUT1 is different from the pathway for $CH_3As(OH)_2$ translocation.

Water permeability and $CH_3As(OH)_2$ uptake are affected in parallel in GLUT1 mutants

Rat GLUT1 exhibits moderate water permeability [24]. Water permeability by wild type and mutant rGLUT1s was examined using an oocyte swelling assay. The P_f values were normalized relative to GLUT1 expression in the plasma membrane, as determined by quantitative immunoblotting (Fig. 8A). The rates of $CH_3As(OH)_2$ uptake were measured in the same batch of oocytes (Fig. 8B) The P_f values of each mutant increased in direct proportion with the rate of $CH_3As(OH)_2$ uptake (Fig. 8C), consistent with our hypothesis that $CH_3As(OH)_2$ and water use the same translocation pathway in GLUT1.

Discussion

Glucose permeases are essential plasma membrane transporters that facilitate the majority of glucose uptake in nearly every mammalian tissue [46]. The GLUT1 isoform also catalyzes the adventitious uptake of $CH_3As(OH)_2$, and, to a less extent, $As(OH)_3$, when expressed in yeast or *X. laevis* oocytes [9], which highlights its important roles in both nutrient uptake and arsenic toxicity. It is reasonable to predict that other mammalian glucose permeases would

NIH-PA Author Manuscript

NIH-PA Author Manuscript

NIH-PA Author Manuscript

have a similar function in uptake of the metalloid arsenic. GLUT1 also serves as a weak water transporter [24]. However, the nature of the pathways for transport of multiple substrates in a single permease is not well understood.

The transport results reported here demonstrate that glucose and $CH_3As(OH)_2$ have different translocation properties via GLUT1. The drastic decrease in glucose uptake in mutants S66F and S66Y indicates that a bulky side chain at Ser^{66} may block glucose binding (Fig. 2B), and a hydrophilic environment is not required at this position since replacement of the serine hydroxyl with a hydrophobic side chain did not affect glucose transport (Fig. 2B). However, all mutations in this position increased uptake of arsenic (Fig. 2C). Substitution of other residues for Arg^{126} each decreased glucose uptake, suggesting that an arginine at this position is involved in glucose transport (Fig. 3B). At the same time, substitution of Arg^{126} with a lysine residue produced a dramatic increase in $CH_3As(OH)_2$ transport (Fig. 3C), suggesting that a smaller positive residue could increase the size of the permeation pathway, for water and arsenicals. Thr^{310} has been proposed to form hydrogen bond with glucose at the exofacial side of the binding site [19]. Replacement of Thr^{310} with amino acids containing larger side chains such as phenylalanine, isoleucine or arginine led to decreased transport of glucose, while alterations to small residues such as alanine, serine or valine did not affect glucose transport (Fig. 4B), indicating that the size of this residue alone affects glucose transport. In contrast, all substitutions of Thr^{310} resulted in significant increases in $CH_3As(OH)_2$ uptake (Fig. 4C), quite different from the glucose uptake results, suggesting that conformational changes in the glucose pathway are transmitted to the separate water and arsenical pathway in GLUT1.

Sugar transporters such as the lactose permease (LacY) [47] and Na^+-coupled glucose permease (vSGLT1) [48] use conformational changes to reorient the substrates from one side of the membrane to the other during the transport reaction. Binding of substrates lead to changes from outward- to inward-facing conformations. GLUT1 would similarly be expected to couple conformational change to sugar or arsenical transport. Logically, glucose would be expected to bind to an outward-facing cavity, inducing a conformational change that drives the reorientation of the site to inward-facing. Therefore, an open conformation of GLUT1 is modeled, and the five residues predicted to form hydrogen bonds with glucose are located in a large open cavity to which glucose molecules initially bind (Fig. 1). The Cα-Cα distances between the rGLUT1 and the LacY outwardly-facing models [11] were reasonably similar (Table 2). The arrangement of the helices in the rGLUT1 outwardly-facing model was consistent with the hGLUT1 model proposed by Mueckler and Makepeace [23]. On the other hand, arsenicals appear to bind to a different location than glucose to a site that may be similar to the entrance of the putative water channel. In this model, this secondary pathway is proposed to function as an auxiliary channel for both water and arsenic (Fig. 1). In rGLUT1 model, Ser^{66} and Thr^{310} are located in the putative glucose binding pocket. Therefore, replacement of these two residues to larger amino acids would be predicted to sterically reduce glucose binding and transport, while arsenic transport might not be expected to be affected, as was experimentally observed (Fig. 2 and 4). The S66F and T310I mutations have been shown to increase water permeation, and also increase arsenical uptake (Fig. 8B). Although a homology model can only provide limited accuracy, it provides testable predictions for further exploration. For examples, the functions of residues that line the putative auxiliary channel, including residues from helix 2, 3, and 4, in arsenical and water transport in future experiments, which may also give insight into ways to decrease uptake of arsenicals without reducing normal sugar transport function.

In solution, trivalent arsenic has tetrahedral structure that mimics water and glycerol [49] but is much smaller than glucose, so it is reasonable to speculate that it binds to a different site than glucose. If they do not compete for the same initial binding site, arsenic and glucose

NIH-PA Author Manuscript

NIH-PA Author Manuscript

NIH-PA Author Manuscript

should inhibit each other non-competitively, as has been observed [9]. In further support of this idea, transport of glucose and arsenic are affected differently by inhibitors such as Hg(II), cytB or forskolin. Hg(II) is proposed to bind Cys^{429} in GLUT1, which is the only cysteine with a thiolate exposed from the exofacial side of the permease [44] (Fig. 1). Binding of this impermeable thiol-reactive reagent at the extracellular surface inhibits glucose transport, but not $CH_3As(OH)_2$ uptake (Fig. 7). Forskolin and glucose are predicted to dock at near each other on the extracellular face of the GLUT1. Forskolin binds near Trp^{65} in the exofacial cavity but also penetrates the plasma membrane and binds to an alternate site near Phe^{81} on the intracellular face of the permease [40]. The precise site of cytB binding is not known but is proposed to dock at the outer face further down the large open cavity than forskolin [40]. None of these inhibitors of glucose uptake affected $CH_3As(OH)_2$ uptake (Fig. 6B).

In summary, preponderance of evidence point to different routes for these two through GLUT1.Adventitious transport of arsenicals via a nutrient transporter makes accumulation of these toxic substances unavoidable. However, identifying the differences in their translocation mechanisms offers the possibility of designing ways to prevent entry of this environmental toxin while allowing uptake of glucose.

Acknowledgments

This work is supported by National Institutes of Health Grant GM55425 to B.P.R. and ES016856 to Z.L.

Abbreviations

GLUT1	glucose transporter isoform 1
$As(OH)_3$	inorganic arsenite
$CH_3As(OH)_2$	methylarsenite
P_f	osmotic water permeability
cytB	cytochalasin B
DMSO	dimethyl sulfoxide
GLUT1-DS	GLUT1-deficiency syndrome

References

1. Abernathy CO, Thomas DJ, Calderon RL. J Nutr. 2003; 133:1536S–1538S. [PubMed: 12730460]
2. Nordstrom DK. Science. 2002; 296:2143–2145. [PubMed: 12077387]
3. Alam MG, Allinson G, Stagnitti F, Tanaka A, Westbrooke M. Int J Environ Health Res. 2002; 12:235–253. [PubMed: 12396524]
4. Weinhold B. Environ Health Perspect. 2004; 112:A880–A887. [PubMed: 15531422]
5. Liu Z, Styblo M, Rosen BP. Environ Health Perspect. 2006; 114:527–531. [PubMed: 16581540]
6. Liu Z, Shen J, Carbrey JM, Mukhopadhyay R, Agre P, Rosen BP. Proc Natl Acad Sci U S A. 2002; 99:6053–6058. [PubMed: 11972053]
7. Marger MD, Saier MH Jr. Trends in biochemical sciences. 1993; 18:13–20. [PubMed: 8438231]
8. Vannucci SJ, Maher F, Simpson IA. Glia. 1997; 21:2–21. [PubMed: 9298843]
9. Liu Z, Sanchez MA, Jiang X, Boles E, Landfear SM, Rosen BP. Biochem Biophys Res Commun. 2006; 351:424–430. [PubMed: 17064664]
10. Huang Y, Lemieux MJ, Song J, Auer M, Wang DN. Science. 2003; 301:616–620. [PubMed: 12893936]

NIH-PA Author Manuscript

NIH-PA Author Manuscript

NIH-PA Author Manuscript

11. Smirnova I, Kasho V, Choe JY, Altenbach C, Hubbell WL, Kaback HR. Proc Natl Acad Sci U S A. 2007; 104:16504–16509. [PubMed: 17925435]
12. Heinze M, Monden I, Keller K. Biochemistry. 2004; 43:931–936. [PubMed: 14744136]
13. Olsowski A, Monden I, Krause G, Keller K. Biochemistry. 2000; 39:2469–2474. [PubMed: 10704196]
14. Mueckler M, Roach W, Makepeace C. J Biol Chem. 2004; 279:46876–46881. [PubMed: 15308632]
15. Mueckler M, Makepeace C. J Biol Chem. 2005; 280:39562–39568. [PubMed: 16172126]
16. Mueckler M, Makepeace C. J Biol Chem. 1999; 274:10923–10926. [PubMed: 10196171]
17. Mueckler M, Makepeace C. J Biol Chem. 2008; 283:11550–11555. [PubMed: 18245775]
18. Hruz PW, Mueckler MM. J Biol Chem. 1999; 274:36176–36180. [PubMed: 10593902]
19. Mueckler M, Makepeace C. J Biol Chem. 2004; 279:10494–10499. [PubMed: 14688257]
20. Mueckler M, Makepeace C. J Biol Chem. 2002; 277:3498–3503. [PubMed: 11713254]
21. Hruz PW, Mueckler MM. Biochemistry. 2000; 39:9367–9372. [PubMed: 10924131]
22. Mueckler M, Makepeace C. J Biol Chem. 2006; 281:36993–36998. [PubMed: 17020877]
23. Mueckler M, Makepeace C. Biochemistry. 2009; 48:5934–5942. [PubMed: 19449892]
24. Fischbarg J, Kuang KY, Vera JC, Arant S, Silverstein SC, Loike J, Rosen OM. Proc Natl Acad Sci U S A. 1990; 87:3244–3247. [PubMed: 2326282]
25. Iserovich P, Wang D, Ma L, Yang H, Zuniga FA, Pascual JM, Kuang K, De Vivo DC, Fischbarg J. J Biol Chem. 2002; 277:30991–30997. [PubMed: 12032147]
26. De Vivo DC, Trifiletti RR, Jacobson RI, Ronen GM, Behmand RA, Harik SI. N Engl J Med. 1991; 325:703–709. [PubMed: 1714544]
27. Liu Z, Boles E, Rosen BP. J Biol Chem. 2004; 279:17312–17318. [PubMed: 14966117]
28. Preston GM, Carroll TP, Guggino WB, Agre P. Science. 1992; 256:385–387. [PubMed: 1373524]
29. Carbrey JM, Cormack BP, Agre P. Yeast. 2001; 18:1391–1396. [PubMed: 11746601]
30. Eswar N, Webb B, Marti-Renom MA, Madhusudhan MS, Eramian D, Shen MY, Pieper U, Sali A. Curr Protoc Protein Sci. 2007; Chapter 2(Unit 29)
31. Brooks BR, Bruccoleri RE, Olafson BD, States DJ, Swaminathan S, Karplus M. J. Comp. Chem. 1983; 4:187–217.
32. Petrek M, Otyepka M, Banas P, Kosinova P, Koca J, Damborsky J. BMC Bioinformatics. 2006; 7:316. [PubMed: 16792811]
33. DeLano WL. http://www.pymol.org.
34. Wang D, Kranz-Eble P, De Vivo DC. Hum Mutat. 2000; 16:224–231. [PubMed: 10980529]
35. Klepper J, Willemsen M, Verrips A, Guertsen E, Herrmann R, Kutzick C, Florcken A, Voit T. Hum Mol Genet. 2001; 10:63–68. [PubMed: 11136715]
36. Brockmann K, Wang D, Korenke CG, von Moers A, Ho YY, Pascual JM, Kuang K, Yang H, Ma L, Kranz-Eble P, Fischbarg J, Hanefeld F, De Vivo DC. Ann Neurol. 2001; 50:476–485. [PubMed: 11603379]
37. Klepper J, Wang D, Fischbarg J, Vera JC, Jarjour IT, O'Driscoll KR, De Vivo DC. Neurochem Res. 1999; 24:587–594. [PubMed: 10227690]
38. Klepper J, Voit T. Eur J Pediatr. 2002; 161:295–304. [PubMed: 12029447]
39. Takata K, Hirano H, Kasahara M. Int Rev Cytol. 1997; 172:1–53. [PubMed: 9102392]
40. Salas-Burgos A, Iserovich P, Zuniga F, Vera JC, Fischbarg J. Biophys J. 2004; 87:2990–2999. [PubMed: 15326030]
41. Dwyer DS. Proteins. 2001; 42:531–541. [PubMed: 11170207]
42. Pascual JM, Wang D, Yang R, Shi L, Yang H, De Vivo DC. J Biol Chem. 2008; 283:16732–16742. [PubMed: 18387950]
43. Lostao MP, Hirayama BA, Panayotova-Heiermann M, Sampogna SL, Bok D, Wright EM. FEBS Lett. 1995; 377:181–184. [PubMed: 8543046]
44. Wellner M, Monden I, Keller K. Biochem J. 1994; 299(Pt 3):813–817. [PubMed: 8192671]
45. Savage DF, Stroud RM. J. Mol. Biol. 2007; 368:607–617. [PubMed: 17376483]

NIH-PA Author Manuscript

NIH-PA Author Manuscript

NIH-PA Author Manuscript

46. Joost HG, Thorens B. Mol Membr Biol. 2001; 18:247–256. [PubMed: 11780753]
47. Abramson J, Smirnova I, Kasho V, Verner G, Kaback HR, Iwata S. Science. 2003; 301:610–615. [PubMed: 12893935]
48. Faham S, Watanabe A, Besserer GM, Cascio D, Specht A, Hirayama BA, Wright EM, Abramson J. Science. 2008; 321:810–814. [PubMed: 18599740]
49. Ramírez-Solis A, Mukopadhyay R, Rosen BP, Stemmler TL. Inorg Chem. 2004; 43:2954–2959. [PubMed: 15106984]

NIH-PA Author Manuscript
NIH-PA Author Manuscript
NIH-PA Author Manuscript

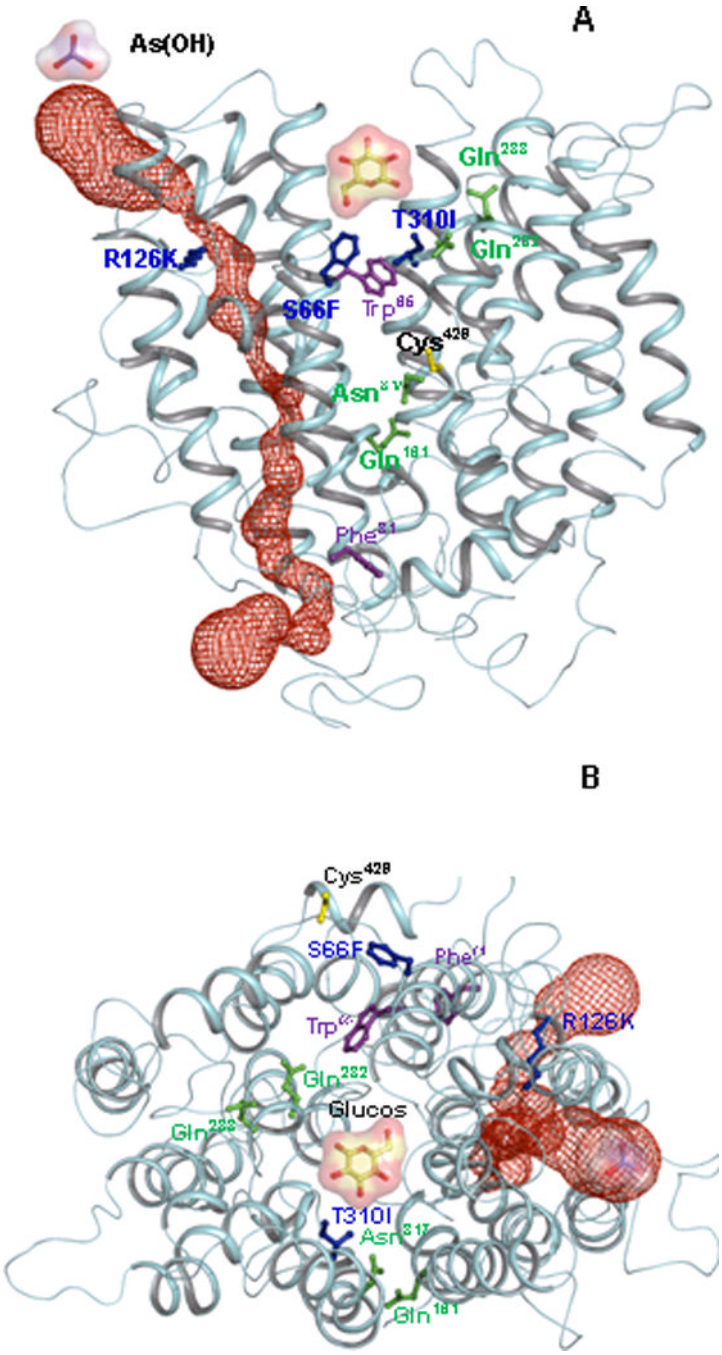

Fig. 1. GLUT1 homology model

Helices are rendered as Cα worms, colored cyan. (A) View from within the plane of the membrane, with the exofacial side at top and cytosollic side at bottom. In this open form, the glucose binding site is shown as a cavity, (B) Exofacial view of the open form of GLUT1. Selected residues are shown in ball and stick: Gln^{161}, Gln^{282}, Gln^{283} and Asn^{317} are shown in green. The GLUT1-DS mutants S66F, R126K, T310I are shown in blue. Cys^{429}, the site of Hg(II) binding, is shown in yellow. Trp^{65} and Phe^{81}, which are the extra- and intracellular forskolin binding sites, respectively, are shown in magenta. The auxiliary (red) channel is shown as space filling representation. Glucose and $As(OH)_3$ molecules are illustrated as ball-and-stick with molecular surface representations.

NIH-PA Author Manuscript
NIH-PA Author Manuscript
NIH-PA Author Manuscript

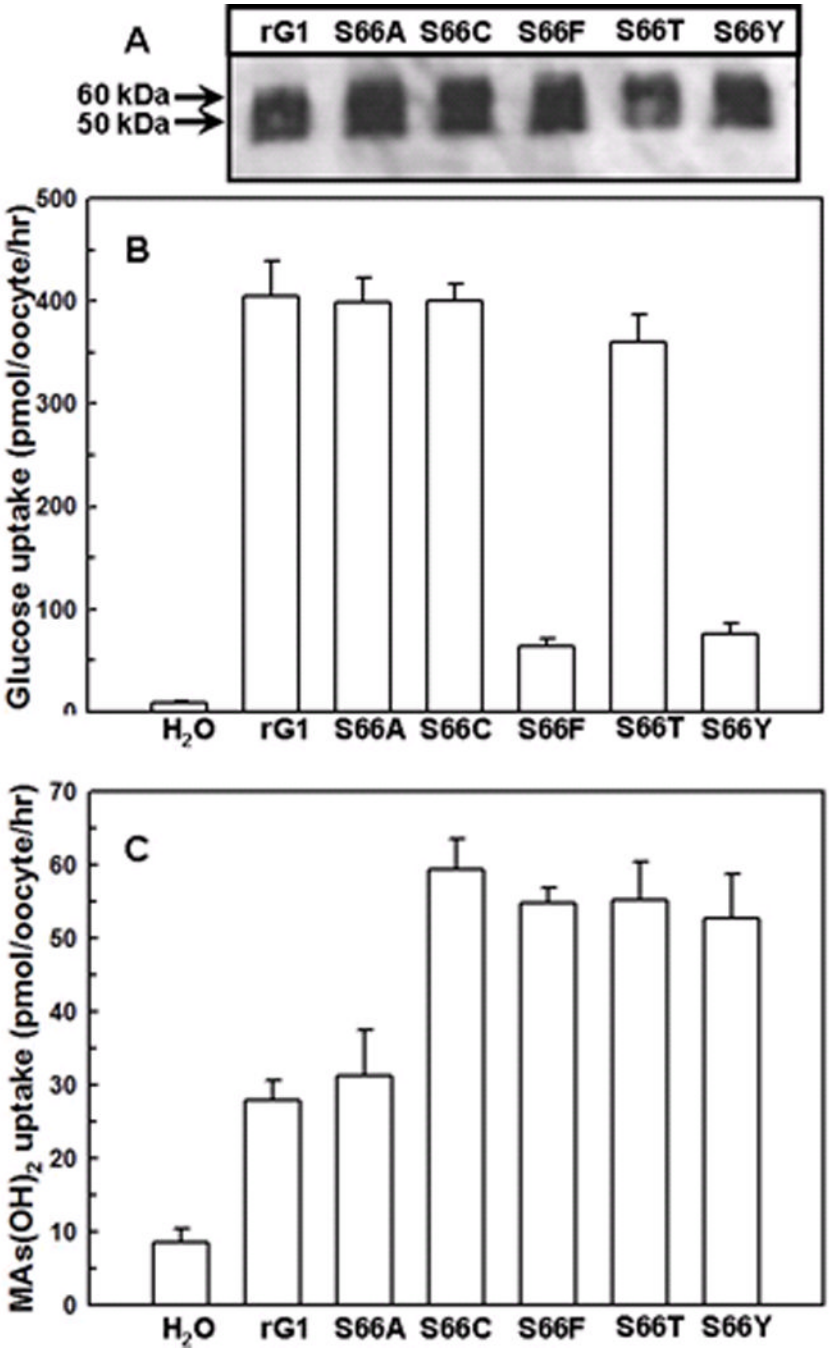

Fig. 2. Transport of glucose and $CH_3As(OH)_2$ via GLUT1 and Ser^{66} mutants

(A) Western blotting results of GLUT1 and Ser^{66} mutants. Membranes of oocytes were prepared as described under Methods. (B) Transport of D-[U-^{14}C] glucose in oocytes expressing GLUT1 and Ser^{66} mutants, along with a water injected control. Glucose was used at a final concentration of 0.1 mM. (C) Transport of $CH_3As(OH)_2$ in oocytes expressing GLUT1 and Ser^{66} mutants, along with a water injected control. $CH_3As(OH)_2$ was used at a final concentration of 0.1 mM. The values in each plot are means of two independent assays.

NIH-PA Author Manuscript

NIH-PA Author Manuscript

NIH-PA Author Manuscript

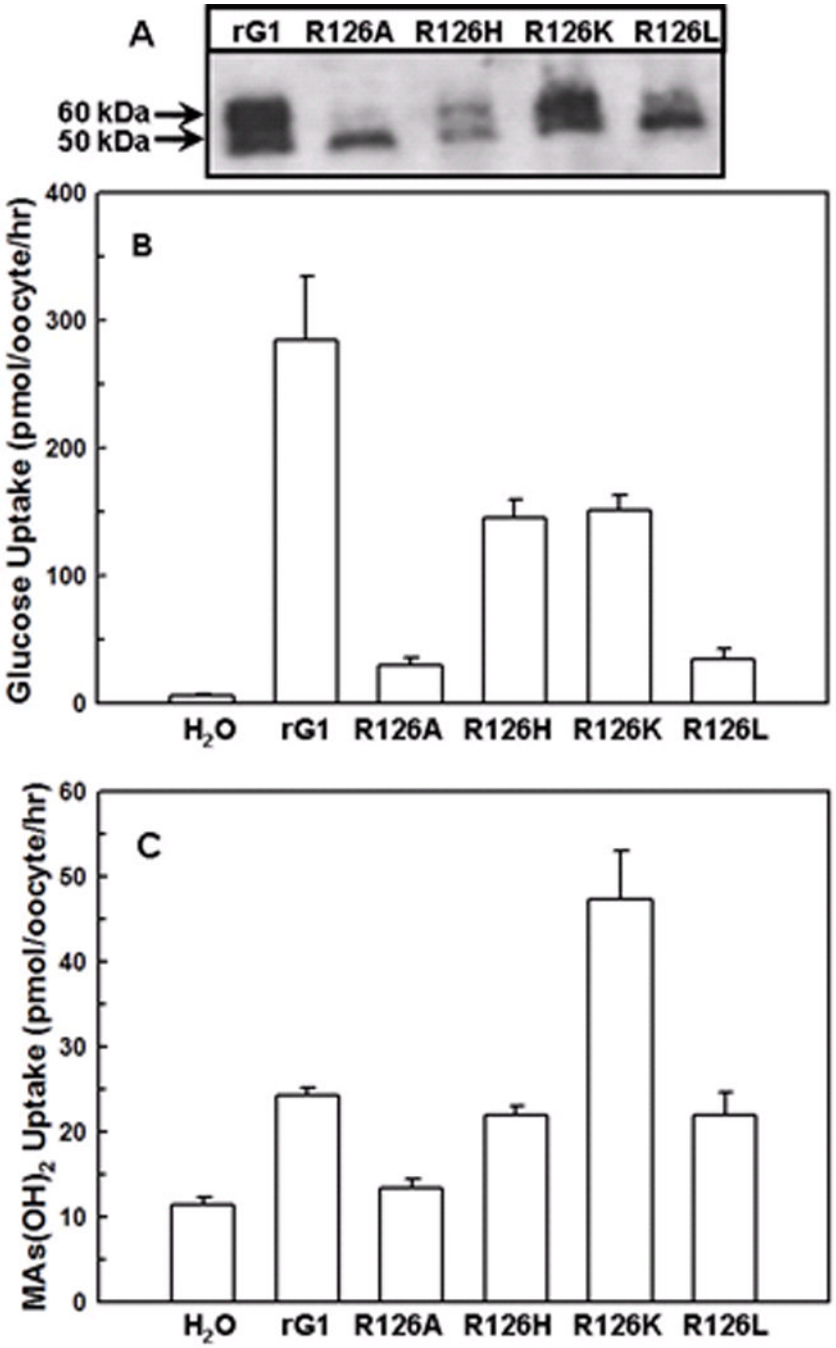

Fig. 3. Transport of glucose and $CH_3As(OH)_2$ via GLUT1 and Arg^{126} mutants

(A) Western blot analysis of rGLUT1 and Arg^{126} mutants expressed in oocyte membranes was probed with an anti-GLUT1 primary antibody. (B) Transport of 0.1 mM D-[U-^{14}C]glucose in oocytes expressing GLUT1 and Arg^{126} mutants, along with a water injected control. (C) Transport of 0.1 mM $CH_3As(OH)_2$ in oocytes expressing GLUT1 and Arg^{126} mutants, along with a water injected control. The values in each plot are means of two independent assays.

NIH-PA Author Manuscript

NIH-PA Author Manuscript

NIH-PA Author Manuscript

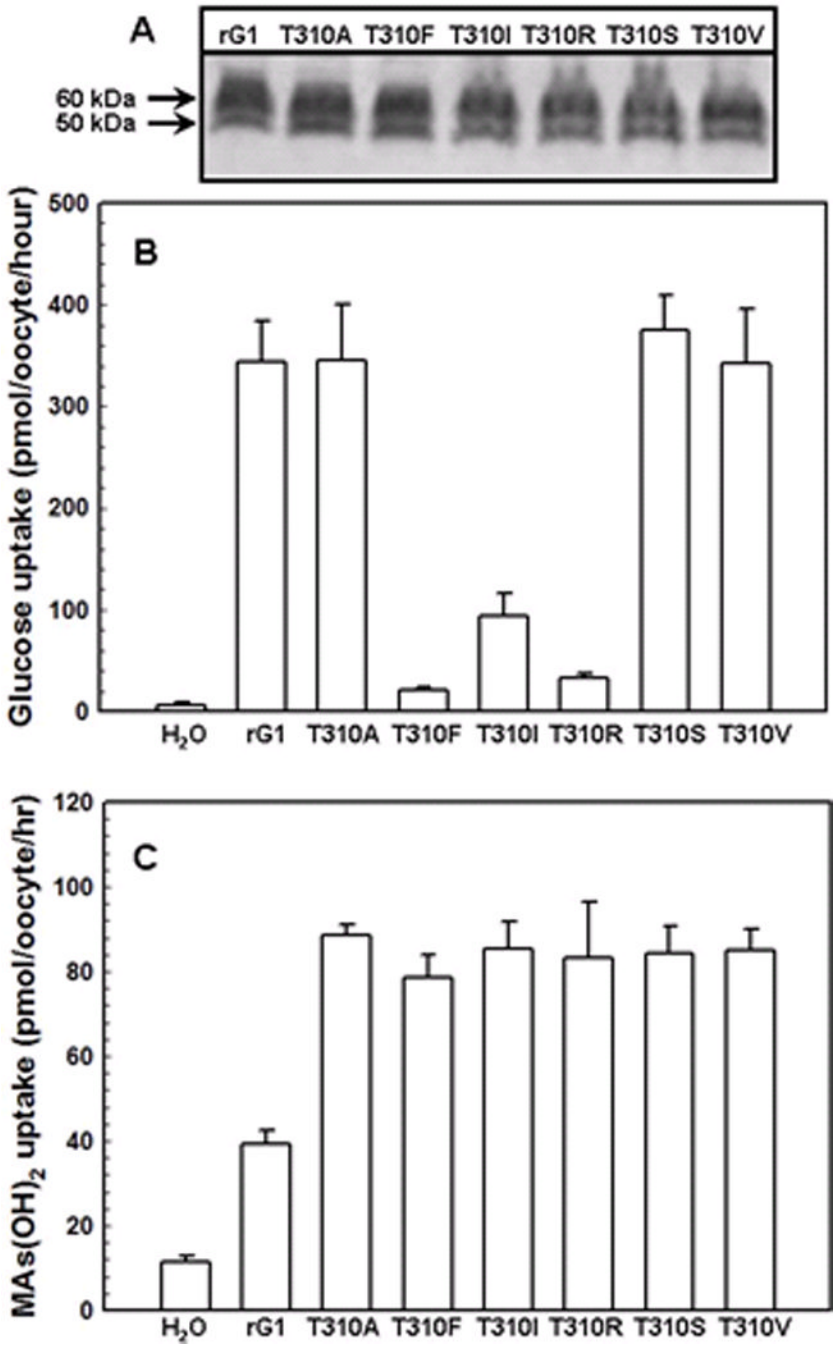

Fig. 4. Transport of glucose and $CH_3As(OH)_2$ via GLUT1 and Thr^{310} mutants

(A) Western blot analysis of rGLUT1 and Thr^{310} mutants expressed in oocyte membranes was probed with an anti-GLUT1 primary antibody. (B) Transport of 0.1 mM D-[U-^{14}C]glucose in oocytes expressing GLUT1 and Thr^{310} mutants, along with a water injected control. (C) Transport of 0.1 mM $CH_3As(OH)_2$ in oocytes expressing GLUT1 and Thr^{310} mutants, along with a water injected control. The values in each plot are means of two independent assays.

NIH-PA Author Manuscript
NIH-PA Author Manuscript
NIH-PA Author Manuscript

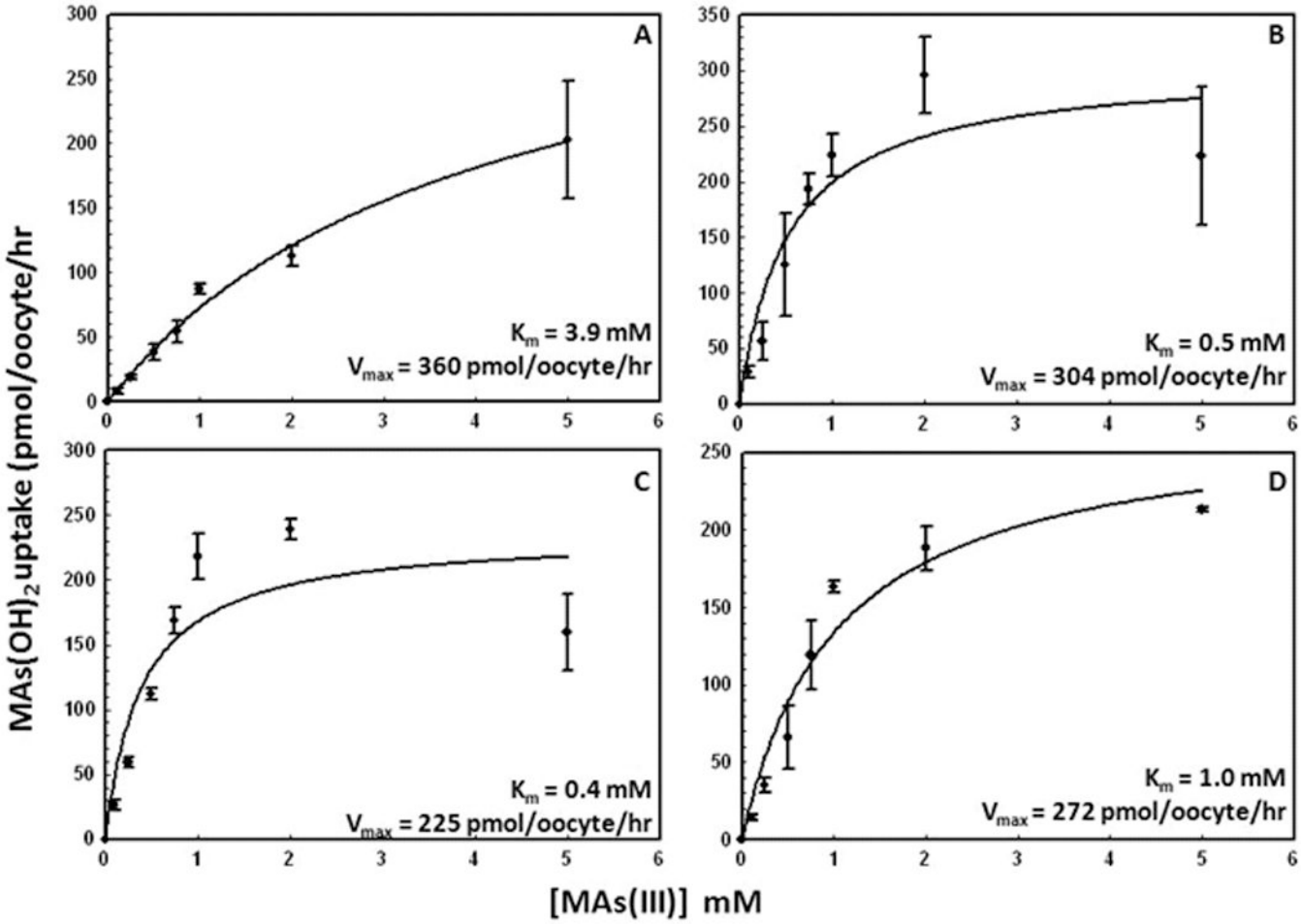

Fig. 5. Kinetic analysis of $CH_3As(OH)_2$ uptake by (A) rGLUT1, (B) S66F, (C) R126K, and (D) T310I

Kinetic parameters were calculated from $CH_3As(OH)_2$ uptake in oocytes expressing rGLUT1 or its mutants after subtraction of uptake in oocytes injected with water. Uptake assays in oocytes were assayed after 30 min of incubation with the indicated concentrations of $CH_3As(OH)_2$. The values in each plot are means of two independent assays. The kinetic parameters were calculated using Sigma Plot 9.0.

NIH-PA Author Manuscript

NIH-PA Author Manuscript

NIH-PA Author Manuscript

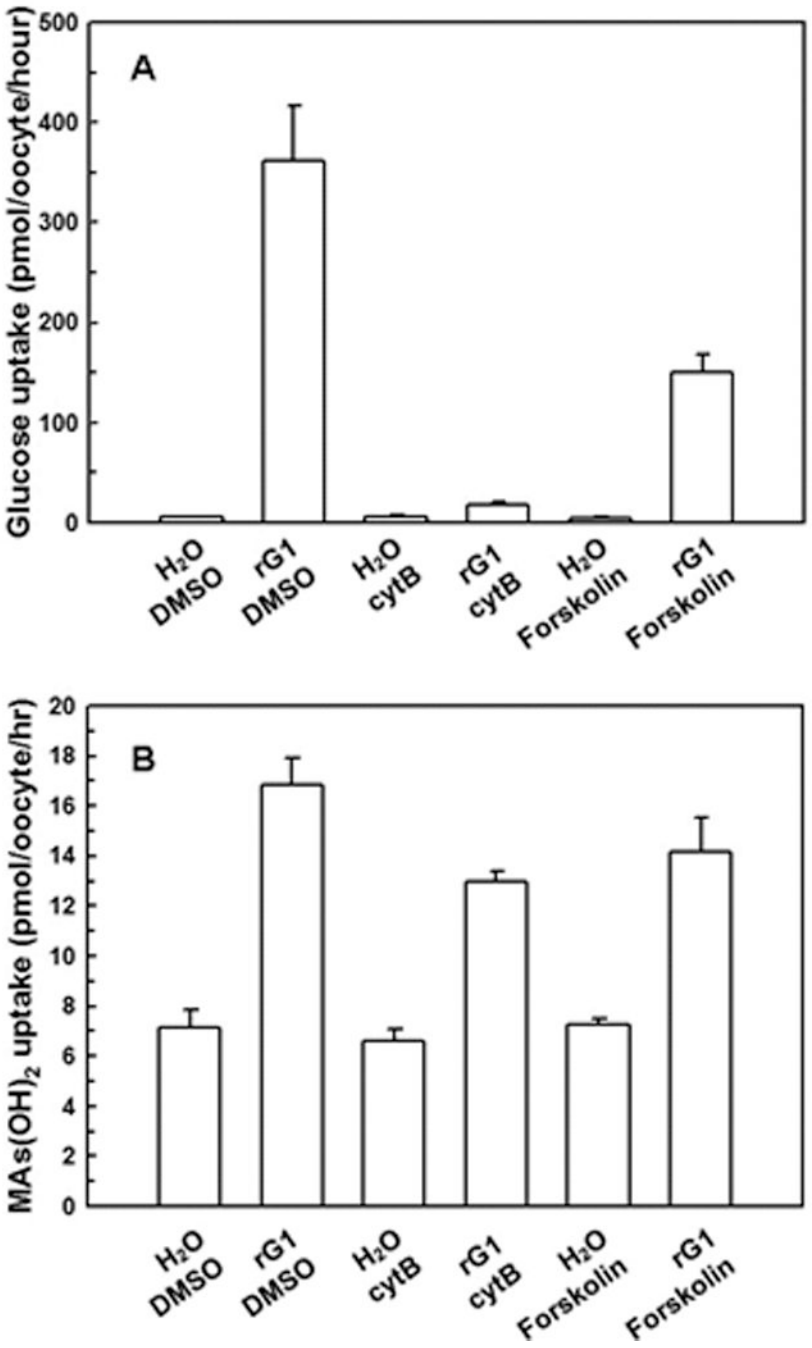

Fig. 6. Inhibition of glucose and $CH_3As(OH)_2$ via rGLUT1 by GLUT inhibitors

(A) Transport of glucose was inhibited by cytB and forskolin in oocytes injected with rGLUT1 cRNA. (B) Transport of MAs(III) was barely affected by cytB and forskolin in oocytes injected with rGLUT1 cRNA. The values in each plot are means of three independent assays.

NIH-PA Author Manuscript

NIH-PA Author Manuscript

NIH-PA Author Manuscript

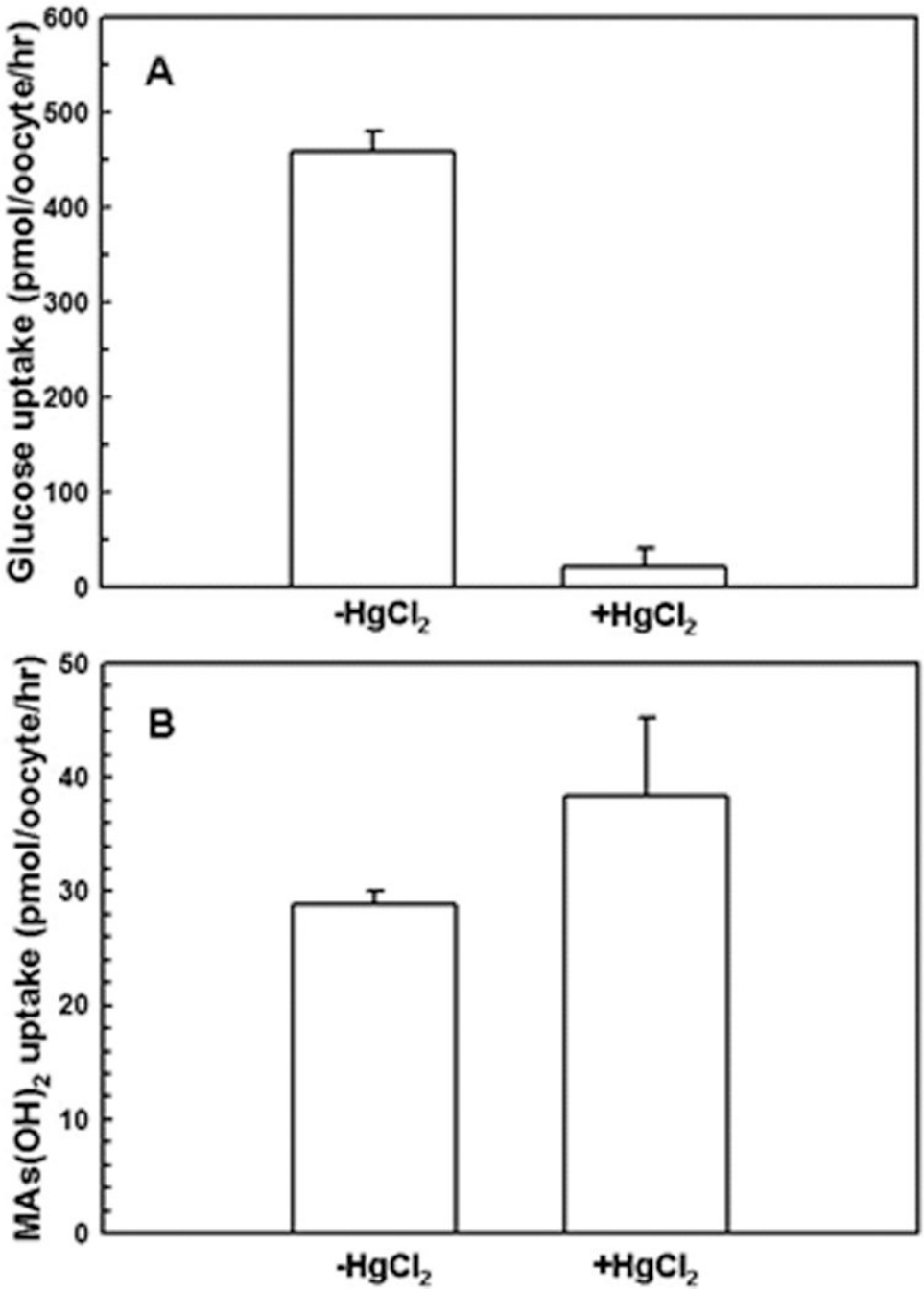

Fig. 7. Inhibition of glucose and $CH_3As(OH)_2$ via rGLUT1 by $HgCl_2$

(A) Transport of glucose by oocytes expressing rGLUT1 after 20-min incubation with $HgCl_2$ was calculated after subtraction of the rates from water-injected oocytes. (B) Transport of $CH_3As(OH)_2$ by oocytes expressing rGLUT1 after 20-min incubation with $HgCl_2$ was calculated after subtraction of the rates from water-injected oocytes. The values in each plot are means of three independent assays.

NIH-PA Author Manuscript
NIH-PA Author Manuscript
NIH-PA Author Manuscript

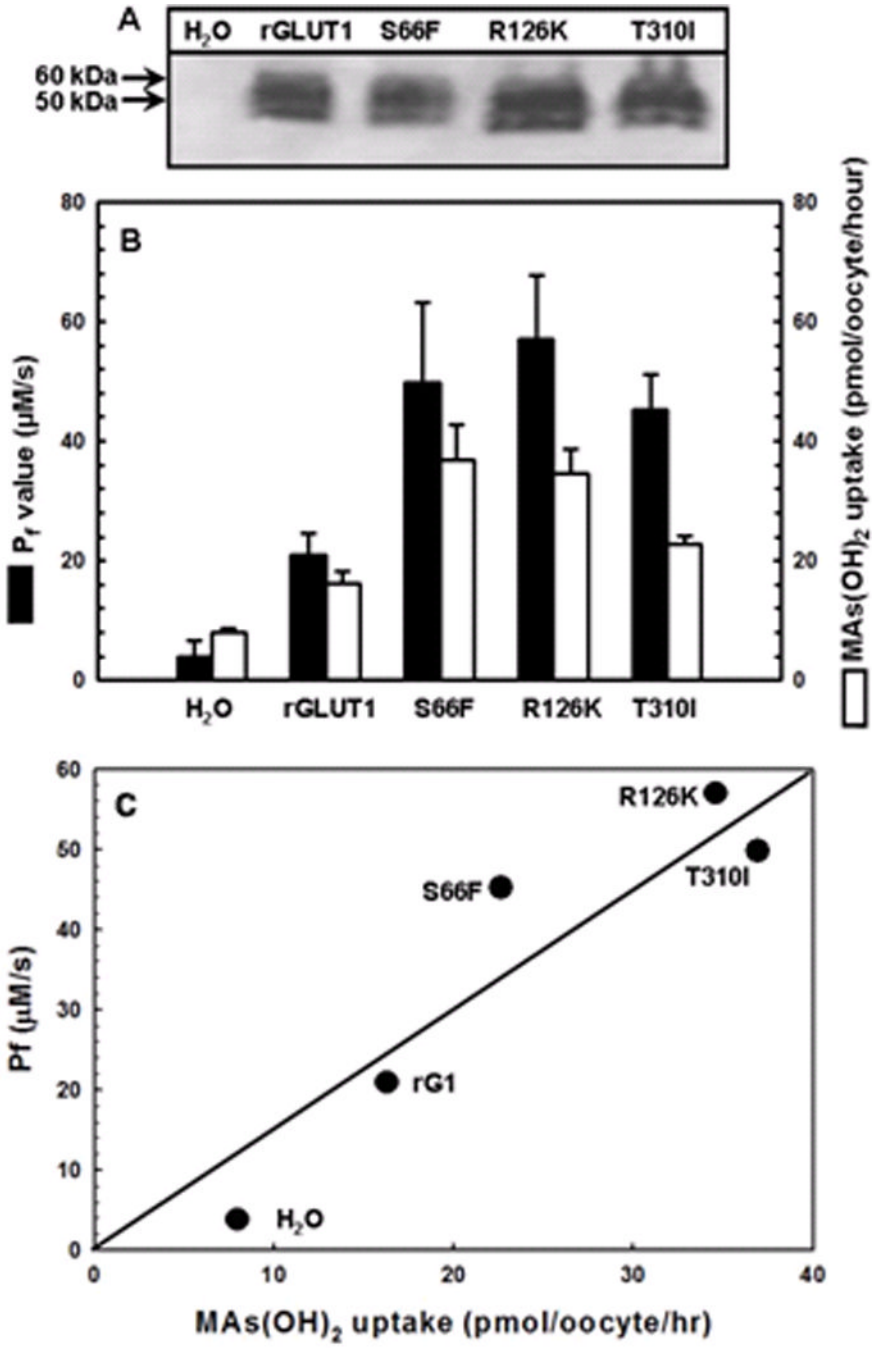

Fig. 8. Correlation between $CH_3As(OH)_2$ uptake (■) and osmotic water permeability (P_f) (□) for oocytes expressing rGLUT1 and its mutants

(A) Western blot analysis of rGLUT1 and its mutants expressed in the oocyte membrane was probed with an anti-GLUT1 primary antibody. (B) P_f values were measured by transferring oocytes into 1:5 diluted ND96 buffer. Swelling assays were performed at room temperature for 1 min. $CH_3As(OH)_2$ transport was assayed with the same batch of oocytes. The values in each plot are means of two independent assays. (C) Correlation of P_f values with $CH_3As(OH)_2$ uptake using the data from (B).

NIH-PA Author Manuscript
NIH-PA Author Manuscript
NIH-PA Author Manuscript

Table 1

Mutagenic oligonucleotides for construction of Ser66, Arg126, and Thr310 mutants of rGLUT1.

Residues	Amino Acid Change	Mutagenic Oligonucleotide
Ser66	Ser→Ala	CTCACCACACTCTGG**GCG**CTCTCCGTGGCCATC
	Ser→Cys	CTCACCACACTCTGG**TGC**CTCTCCGTGGCCATC
	Ser→Phe	CTCACCACACTCTGG**TTT**CTCTCCGTGGCCATC
	Ser→Thr	CTCACCACACTCTGG**ACC**CTCTCCGTGGCCATC
	Ser→Tyr	CTCACCACACTCTGG**TAT**CTCTCCGTGGCCATC
Arg126	Arg→Ala	ATGCTGATCCTGGGC**GCG**TTCATCATTGGAGTG
	Arg→His	ATGCTGATCCTGGGC**CAT**TTCATCATTGGAGTG
	Arg→Lys	ATGCTGATCCTGGGC**AAA**TTCATCATTGGAGTG
	Arg→Leu	ATGCTGATCCTGGGC**CTG**TTCATCATTGGAGTG
Thr310	Thr→Ala	CAGCCTGTGTATGCC**GCG**ATCGGCTCGGGTATC
	Thr→Phe	CAGCCTGTGTATGCC**TTT**ATCGGCTCGGGTATC
	Thr→Ile	CAGCCTGTGTATGCC**ATT**ATCGGCTCGGGTATC
	Thr→Arg	CAGCCTGTGTATGCC**CGT**ATCGGCTCGGGTATC
	Thr→Ser	CAGCCTGTGTATGCC**TCT**ATCGGCTCGGGTATC
	Thr→Val	CAGCCTGTGTATGCC**GTG**ATCGGCTCGGGTATC

NIH-PA Author Manuscript
NIH-PA Author Manuscript
NIH-PA Author Manuscript

Table 2

The Cα-Cα distance compared between the rat GLUT1 outward model and LacY outward model

LacY model (ref)			GLUT1 model (Current Study)		
Pair of Residues	**Inward-facing crystal structure (1PV6) Cα-Cα,Å**	**Outward-facing model Cα-Cα, Å**	**Pair of Residues**	**Inward-facing model Cα-Cα, Å**	**Outward-facing model Cα-Cα, Å**
73–401	41	27	86–475	41	32
73–340	36	21	86–401	36	25
136–340	34	17	152–401	35	17
137–340	32	16	153–401	35	17
136–401	40	24	152–475	41	23
137–401	38	22	153–475	37	22
105–310	34	41	116–357	34	46
164–310	27	43	180–357	30	43
164–375	33	49	180–447	33	48